

Origins of Distinctly Different Behaviors of Pd and Pt Contacts on Graphene

Q. J. Wang and J. G. Che*

Surface Physics Laboratory (National Key Laboratory) and Department of Physics, Fudan University, Shanghai 200433, People's Republic of China

(Received 9 February 2009; published 6 August 2009)

Based on first-principles calculations, we propose an exchange-transfer mechanism to understand the distinctively different behaviors of Pd and Pt contacts on graphene. The feature of the mechanism is that the π electrons on the graphene transferring to the Pd $d_{xz} + d_{yz}$ orbital are largely compensated by the electrons from the Pd d_{z^2} orbital. This mechanism causes more interaction states and transmission channels between the Pd and graphene. Most importantly, the mechanism keeps enough π electrons on the graphene. We show that a tensile strain in the Pd layer, necessary to match the graphene lattice, plays a key role in stimulating this exchange transfer when Pd covers on graphene, while a similar strain in the Pt layer does not cause such a mechanism.

DOI: [10.1103/PhysRevLett.103.066802](https://doi.org/10.1103/PhysRevLett.103.066802)

PACS numbers: 73.63.Rt, 31.15.A-, 73.40.Cg, 73.40.Ns

A key problem for improving performance of electronic devices is reducing or eliminating the electronic barrier into devices, specifically for nanoelectronic devices made by nanomaterials such as carbon nanotubes (CNT) [1]. It was reported by Javey *et al.* [2] that by choosing the correct combination of metal and CNT, the barrier could be effectively reduced. They found that a ballistic transmission between Pd and semiconducting single-walled carbon nanotubes (SWNT) with a wide diameter (3 nm) can be achieved. The same group also found that Pd has an Ohmic contact on metallic SWNTs [3]. In contrast, however, Pt forms a non-Ohmic contact when coating on either semiconducting or metallic SWNTs [2,3]. A question has thus been posed since that time: why do the two metals with electronic isostructures have such a different behavior when coating on CNTs [4].

Because of its importance for low resistance contacts to nanotubes from both technology and fundamental aspects of the nanoelectronic devices, the question has stimulated much effort to clarify the physics [1,3,5–10]. Compared with other metals such as Ti, Au, Ni, Nb, and Al coating on CNTs, a conventional understanding is that the low barrier between Pd and CNT may be traced to the high work function of Pd (5.1 eV) [2]. However, Pt has a higher work function (5.7 eV) [2]. The barrier heights of metal (Au, Pd, Pt) and semiconducting (8,0) SWNT junction were calculated by Shan and Cho [5]. They found that Pd SWNT has the lowest barrier height, however, only 0.1 eV lower than that of Pt. Based on first-principles calculations, five metals (Ti, Pd, Pt, Cu, and Au) contact with SWNT were studied by Matsuda *et al.* [10] and they found that Ti leads to the lowest contact resistance, which is in contrast to the experiments [1].

The observation by Javey *et al.* [2] still remains to be understood. This observation is of experimental nature to underline the importance of a thorough theoretical investigation. In theoretical aspects, however, simulating atoms coating on a CNT is still a challenge. Because of computer

consumption, the contacts between CNTs and electrodes are conventionally simulated by either end contact or side contact. However, metal coated on CNTs should realistically be neither side contact nor end contact; rather, CNTs should be surrounded by metal atoms, a dirty system without translation symmetry. The actual atomic structure at the contact is unclear, perhaps due to the change from sample to sample for fabricating. Therefore, it is instructive to extract the different interaction involved when Pd and Pt are coated on CNTs from various effects. As a first attempt, we study the contact of Pd and Pt on graphene instead of on CNTs, in order to circumvent the difficulty for modeling the contact of metal coating on CNTs and to provide a useful guidance for interpreting the experiments. On the other hand, as an unrolled CNT, the graphene itself is also a rapidly rising star of the family of carbon nanomaterials with interesting electronic, thermal, and mechanical properties for potential applications and technological advance in electronic device miniaturization [11]. Those contacts with electrodes are also critically important and have attracted increasing attention.

Based on first-principles calculations, we propose in this Letter an exchange-transfer mechanism to understand the distinctively different behaviors of Pd and Pt contacts on graphene. Our calculations were performed under the framework of density functional theory as implemented in the VASP package [12]. Electron-ion interactions were described by the projector augmented plane wave method [13], and the wave functions were expanded in a plane wave basis set with an energy cutoff of 500 eV. The k points in the two-dimensional Brillouin zone were sampled on a 16×16 mesh. It is well established that the local density approximation (LDA) [14] for the exchange-correlation interaction underestimates the distance for the van der Waals interaction, while the general gradient approximation (GGA) [15] overestimates it. We find that the LDA gives rise to a graphite layer space of 3.34 Å, in good agreement with the experimental value, while the GGA

leads to a layer space of 4.64 Å. Using the LDA, we calculated multilayer relaxations for Pd and Pt(111) surface. The layer relaxations of the topmost five layers for Pt(111) are +0.68%, -0.45%, -0.30%, +0.03%, +0.14%, respectively, while for Pd(111), the layer relaxation of the topmost layer is +0.30%. These layer relaxations are in good agreement with that obtained by the GGA in recent work [16]. Thus, we adopt the LDA in our calculations. The calculated lattice constants of graphene, Pd, and Pt are 2.45, 3.86, and 3.91 Å, respectively, which is consistent with the experimental values, 2.46, 3.89, and 3.91 Å, respectively [17,18]. The calculated bulk moduli of Pd and Pt are 2.22 and 3.02 Mbar, respectively, which also agrees well with the experimental values 1.808 and 2.783 Mbar [18]. In the calculations, the systems were modeled as slabs with several Pd (Pt) atomic layers and one graphene layer, separated by a vacuum of about 16 Å. All atoms are allowed to relax until the Hellman-Feynman forces on the atoms smaller than 0.01 eV/Å.

We first determine the geometric structures of Pd (Pt) depositing on the graphene. We use a $\sqrt{3} \times \sqrt{3}$ unit cell of metals within a fcc structure in the (111) orientation, which forms a hexagonal lattice, to accommodate a 2×2 unit cell of the graphene, a two-dimensional honeycomb structure. This leads to a 3.5% and 2.3% tensile strain (defined as a ratio of the extension compared to its original dimensions in percentage) for Pd and Pt layers, respectively. This unit cell for one metal monolayer (ML) covering on the graphene has three metal atoms and eight carbon atoms. The optimized average distance of the metal to the graphene layer is 2.49 and 3.33 Å for Pd and Pt with the adsorption energy of 0.54 and 0.26 eV per unit cell, respectively. This means that the Pd layer is coupled with the graphene, while the Pt layer is a relatively inert layer. Two of three Pd atoms in the unit cell favor occupying the top site of the graphene, and the other one favors the hollow site, which are noted in the following by using subscripts “top” and “hol.”

To check the thickness effect of the metal layers on the distance, we deposit more metal layers on, which are extended in the (111) orientation of the fcc structure. It is shown that for up to 5 ML, the average distance of the Pd (Pt) and graphene layer at the interface is changed less than 0.25 Å; specifically, the average distances for 2–5 ML Pd on graphene are 2.39, 2.26, 2.35, and 2.30 Å, respectively, while those for 2–5 ML Pt on graphene are 3.19, 3.26, 3.25, and 3.18 Å, respectively, in good agreement with recent calculations [19].

The distance of the contact layers for the Pd and Pt on graphene shows that the contact of Pd and Pt on the graphene is really distinctively different. To understand the physical mechanism, we examine the charge transfer for 1 ML Pd on graphene. Figure 1 shows its charge density difference, defined as $\Delta\rho = \rho_{\text{Pd/graphene}} - \rho_{\text{graphene}} - \rho_{\text{Pd}}$. Here $\rho_{\text{Pd/graphene}}$, ρ_{graphene} , and ρ_{Pd} represent the charge density of the Pd covering on graphene, the graphene layer,

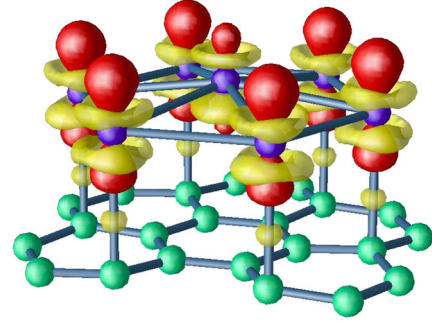


FIG. 1 (color online). Charge transfer for 1 ML Pd on graphene. The blue (darker) and green (lighter) balls represent Pd and C atoms, respectively. The yellow (lighter) and red (darker) isosurfaces ($\pm 4.5 \times 10^{-2} e/\text{\AA}^3$) correspond to electron increase and depletion zone, respectively.

and the Pd freestanding layer, respectively. The yellow (lighter) isosurface corresponds to an electron increase zone, while the red (darker) one is an electron depletion zone. Clearly, the red (darker) distribution around the Pd has the type of the d_{z^2} orbital, while the yellow (lighter) one shows the $d_{xz} + d_{yz}$ component. The charge density difference for 5 ML Pd on graphene shows similar characters, implying that the free surface of the metal multilayer has only small influence in the behaviors of the contact layers.

Analyzing the orbital symmetry one can conclude that electrons transfer between the Pd and graphene layer. The graphene π orbital plays a bridge role in the electron transfer between the Pd and graphene layer. The electrons on the π orbital of graphene transferring to the $d_{xz} + d_{yz}$ orbital of Pd are largely compensated by the electrons on the d_{z^2} orbital of Pd. We denote the mechanism as exchange transfer. Doubtless, this exchange-transfer mechanism increases the interaction states and transmission channels between the Pd and graphene layer. Most importantly, the mechanism keeps enough π electrons on the graphene.

In order to further illustrate the evolution of these states, we display the local density of states (LDOS) of the $d_{xz} + d_{yz}$ orbitals of the Pd contact layer for 1 and 5 ML Pd on the graphene in Figs. 2(a) and 2(b), respectively. In the figure the LDOS of Pd_{top} and Pd_{hol} are represented by solid curves and dashed curves, respectively. As a reference, we also plot the LDOS for the corresponding Pd freestanding layer (dotted curve).

The LDOS for the 1 ML Pd freestanding layer (dotted curve) has two main peaks at about -1.7 and -0.3 eV, respectively. Analyzing the orbital components and electron distribution of these states indicates that the states near -1.7 eV are dominantly hybrids of the $d_{xz} + d_{yz}$ orbitals between the neighboring Pd atoms, which can be identified as bondinglike states, while those near -0.3 eV can be identified as antibondinglike states due to its wave function nodes between the neighboring atoms. The hybrids of the $d_{xz} + d_{yz}$ orbitals are strain-dependent.

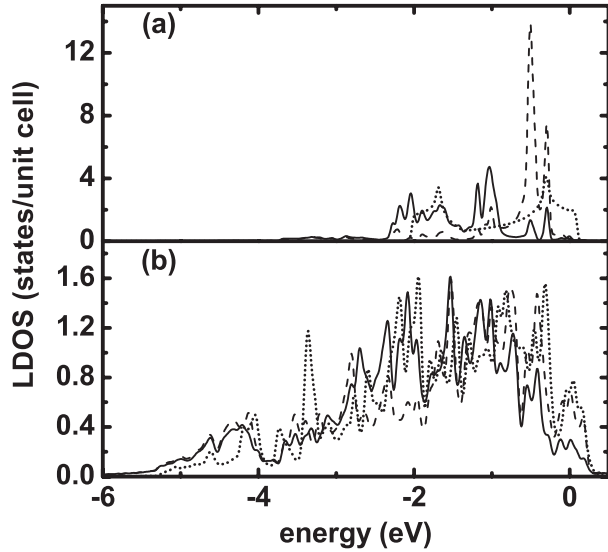


FIG. 2. Local density of states of $d_{xz} + d_{yz}$ orbitals in the contact layer for 1 ML (a) and 5 ML (b) Pd on graphene. The solid curves and the dashed curves are the LDOS of the atoms on the top and hollow sites, respectively. The Fermi energy is set at zero. The corresponding LDOS for the freestanding layer is given by the dotted curves.

We find that the $d_{xz} + d_{yz}$ bands for the 5 ML Pd case are more extended than those for the 1 ML Pd case, as shown in Fig. 2(b). This can be expected. Furthermore, the LDOS for the freestanding 5 ML Pd (dotted curve) has many peaks, which are created by interactions between $d_{xz} + d_{yz}$ orbitals at the surface and interactions between $d_{xz} + d_{yz}$ orbitals at the surface and d orbitals in subsurface. However, the states near -0.81 and -0.30 eV can still be identified as bonding and antibonding states of the $d_{xz} + d_{yz}$ at the surface, respectively. Other main peaks are surface states created by interactions between the surface and the subsurface. When 5 ML Pd are deposited on graphene, the states at -1.15 and -0.71 eV can be identified mainly localized in the Pd contact layer. The features of the interactions for the 1 ML Pd on graphene partly remain for the 5 ML Pd on graphene. These interactions in the contact layer and with the sublayers are also strain-dependent.

Thus we can understand the origin of the interaction between Pd and C: when Pd covers graphene, the π electrons of the graphene transfer to the antibonding states of Pd $d_{xz} + d_{yz}$ orbitals, weakening the bonding states. For 1 ML Pd on graphene, as the interaction between the neighboring Pd atoms decreases, the bonding states near -1.7 eV will move up to -0.5 eV, where a sharp peak appears in the LDOS for Pd_{hol} (dashed curve) in Fig. 2(a). In contrast, the changes of the LDOS for Pd_{top} (solid curve) are not as large, since the Pd_{hol} has six neighboring C atoms within the interaction range of the $d_{xz} + d_{yz}$ orbitals, while the Pd_{top} only has three.

Next, we focus on why Pt on graphene does not behave like Pd on graphene, although the two systems have simi-

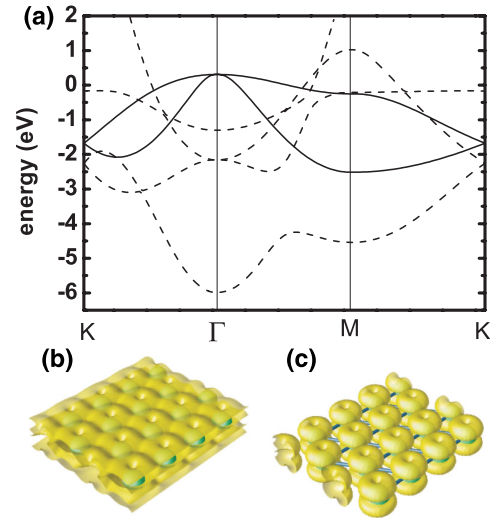


FIG. 3 (color online). Band structures for the freestanding Pt layer (a). Panels (b) and (c) are the electron distribution for the lower and upper band (solid lines) at the M point, respectively. The Fermi energy is set at zero. The isosurface is $3.4 \times 10^{-2} e/\text{\AA}^3$.

lar structures. Figure 3(a) shows the band structures of the freestanding 1 ML Pt with the lattice constant corresponding to that of the graphene. In the figure, two solid curves represent the bands of the $d_{xz} + d_{yz}$ bonding (lower) and antibonding (upper) states, respectively. Figures 3(b) and 3(c) display electron distributions of the lower and upper band at the M point, respectively. The distribution for the bonding states is quite flat, similar to that of the π electrons of graphene. These two electron distributions between Pt and graphene are repulsive. The similar repulsive behaviors between graphite interlayers are also observed [20]. In contrast, the electron distribution of the antibonding states fluctuates, which attracts the π electrons of the graphene. Therefore, the interlayer interaction between Pt and graphene is mainly dominated by the $d_{xz} + d_{yz}$ bonding and antibonding states of Pt, which depend strongly on the strain in the Pt layer due to matching the graphene lattice.

Our calculations show that the peak of the $d_{xz} + d_{yz}$ bonding states of the freestanding 1 ML Pt shifts from -2.31 eV for the 0.0% strain to -2.07 and -1.88 eV for the 2.3% and 4.5% strains, while for the Pd, this peak shifts from -2.01 eV for the 0.0% strain to -1.68 and -1.62 eV for the 3.5% and 4.5% strains. This indicates that with the increase of the tensile strain, the bonding is weakened and thus the chemical reactivity increases. However, it is not favorable for the Pt layer to extend its lattice to match the graphene lattice. It is shown that the calculated surface stress for the freestanding 5 ML Pd to match the graphene lattice is -3.29 eV per 1×1 unit cell, while for the 5 ML Pt the value is -3.76 eV. Furthermore, we find that for the 1 ML Pt on graphene, three Pt atoms in the unit cell shrink to form an equilateral triangle with the bond length of 2.67 \AA, 0.17 \AA smaller than that in bulk Pt with the same

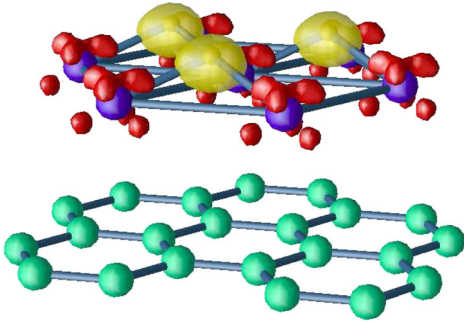


FIG. 4 (color online). The same as Fig. 1, but for depositing H on the Pd layer. The small balls in the yellow (lighter) zone represent H atoms. The isosurface is $\pm 8.2 \times 10^{-2} e/\text{\AA}^3$.

strain of 2.3%. In contrast, for 1 ML Pd on graphene, the distance of $\text{Pd}_{\text{top}}\text{-Pd}_{\text{top}}$ and $\text{Pd}_{\text{top}}\text{-Pd}_{\text{hol}}$ is 2.83 and 2.84 Å, respectively, almost the same as that in bulk with the same strain of 3.5%, 2.83 Å. This fact is consistent with the experimental observations: the Pt forms particles when coating on CNT, while the Pd can continuously grow on CNT due to a strong interaction with CNT [21]. Our calculations show that this contraction begins from 1.0% tensile strain in Pt monolayer, while up to 6.4% tensile strain in Pd monolayer the Pd does not contract, indicating that in quite a wide range of the strain, the interaction competition between Pt-Pt and Pt-C (Pd-Pd and Pd-C) favors the Pt-Pt interaction for Pt/graphene, while it favors the Pd-C interaction for Pd/graphene. As a consequence, due to low reactivity, Pt cannot trigger the exchange transfer in the Pt on graphene.

Now it can be concluded that the key to understand the different behaviors of Pd and Pt contacts on graphene is the hybridization of the $d_{xz} + d_{yz}$ orbitals between the neighboring metal atoms. The strain effect on the reactivity of metal surfaces has also been discussed by Mavrikakis *et al.*, and they concluded that surface reactivity increases with lattice expansion, following a concurrent up-shift of the metal d states [22]. Following this viewpoint, it can be expected that if the hybridization of the $d_{xz} + d_{yz}$ orbitals between the Pd atoms changes strongly enough to favor the interaction of Pd-Pd compared with that of Pd-C, the exchange-transfer mechanism will be suppressed, and the distance of the contact layer between Pd and graphene will thus increase.

In order to confirm this argument, we deposited H on the hollow site of the Pd layer. After full relaxation, the distance of Pd and graphene increases to 3.08 Å. The distance of H to Pd is 1.78 Å, and the height of H to the Pd plane is 0.74 Å. Analyzing the electron distribution indicates that the electrons in the $d_{xz} + d_{yz}$ orbitals of Pd transfer to H atoms, as shown in Fig. 4; that is, the $d_{xz} + d_{yz}$ antibonding orbitals lose electrons, leading to stronger bonding states, thus decreasing the chemical reactivity of the Pd layer and turning off the exchange-transfer mechanism.

In summary, based on first-principles calculations, we showed that the $d_{xz} + d_{yz}$ bonding of the neighboring Pd (Pt) atoms, which depends strongly on the strain in the Pd (Pt) layers, is mainly responsible for the different behaviors of Pd and Pt contacts on graphene. It has been demonstrated that the tensile strain in the Pd layer due to matching the graphene lattice leads to increasing its chemical reactivity, resulting in the electron exchange transfer between the Pd and graphene layer, while a similar strain in the Pt layer could not cause such interactions. The exchange-transfer mechanism increases the interaction states and transmission channels between the Pd and graphene. Most importantly, the mechanism keeps enough π electrons on the graphene for conducting. Since the difference of electronic structures between the graphene and carbon nanotubes is mainly in curvature effects [23], the physical origins may be extended to understand the different contact of Pd and Pt coating on carbon nanotubes and are specifically presumable for Pd and Pt on the CNTs with a large diameter.

This work was supported by the NSFC, MOE, MOST of China (Grants No. 2009CB929203, No. 2006CB921300, and No. 2009ZX02035).

*Corresponding author.

jjgche@fudan.edu.cn.

- [1] H. J. Dai *et al.*, *Nano* **1**, 1 (2006).
- [2] A. Javey *et al.*, *Nature (London)* **424**, 654 (2003).
- [3] D. Mann *et al.*, *Nano Lett.* **3**, 1541 (2003).
- [4] J. Tersoff, *Nature (London)* **424**, 622 (2003).
- [5] B. Shan and K. Cho, *Phys. Rev. B* **70**, 233405 (2004).
- [6] B. Shan and K. Cho, *Phys. Rev. Lett.* **94**, 236602 (2005).
- [7] Z. H. Chen *et al.*, *Nano Lett.* **5**, 1497 (2005).
- [8] A. Maiti and A. Ricca, *Chem. Phys. Lett.* **395**, 7 (2004).
- [9] N. Nemeč *et al.*, *Phys. Rev. Lett.* **96**, 076802 (2006).
- [10] Y. Matsuda *et al.*, *J. Phys. Chem. C* **111**, 11 113 (2007).
- [11] A. K. Geim and K. S. Novoselov, *Nature Mater.* **6**, 183 (2007).
- [12] G. Kresse and J. Hafner, *Phys. Rev. B* **47**, 558 (1993); **49**, 14 251 (1994); G. Kresse and J. Furthmüller, *Comput. Mater. Sci.* **6**, 15 (1996); G. Kresse and J. Furthmüller, *Phys. Rev. B* **54**, 11 169 (1996).
- [13] P. E. Blöchl, *Phys. Rev. B* **50**, 17953 (1994).
- [14] D. M. Ceperley and B. J. Alder, *Phys. Rev. Lett.* **45**, 566 (1980).
- [15] J. P. Perdew and Y. Wang, *Phys. Rev. B* **45**, 13 244 (1992).
- [16] K. Kádás *et al.*, *Surf. Sci.* **600**, 395 (2006); V. Zólyomi *et al.*, *J. Phys. Condens. Matter* **21**, 095007 (2009).
- [17] Y. Baskin and L. Meyer, *Phys. Rev.* **100**, 544 (1955).
- [18] C. Kittel, *Introduction to Solid State Physics* (Wiley, New York, 1996), 7th ed.
- [19] G. Giovannetti *et al.*, *Phys. Rev. Lett.* **101**, 026803 (2008).
- [20] T. Yumura and K. Yoshizawa, *Chem. Phys.* **279**, 111 (2002).
- [21] Y. Zhang and H. J. Dai, *Appl. Phys. Lett.* **77**, 3015 (2000); Y. Zhang *et al.*, *Chem. Phys. Lett.* **331**, 35 (2000).
- [22] M. Mavrikakis *et al.*, *Phys. Rev. Lett.* **81**, 2819 (1998).
- [23] X. Blase *et al.*, *Phys. Rev. Lett.* **72**, 1878 (1994).